Topologically protected surface states in non-centrosymmetric superconductors

A. P. Schnyder, P. M. R. Brydon[1], S. Ryu[2], and C. Timm[1]

The hallmark of topological insulators and superconductors is the existence of topologically protected zero-energy surface or edge states, some of which are of Majorana type. The experimental observation of these edge and surface states in HgTe/(Hg,Ce)Te quantum wells and in BiSb alloys, respectively, has lead to a renewed interest in topological states of matter. Recently, we have shown that topologically protected zero-energy states can also occur at the surface of noncentrosymmetric superconductors [1-3], such as $CePt_3Si$ or $Li_2Pd_xPt_{3-x}B$. In these remarkable materials, Rashba-type antisymmetric spin-orbit interactions lift the spin degeneracy of the electronic bands and generate complex spin textures in the electron Bloch functions. In the superconducting state, the antisymmetric spin-orbit coupling gives rise to the admixture of even-parity spin-singlet and odd-parity spin-triplet pairing components and, importantly, allows a non-trivial topology of the Bogoliubov-quasiparticle wavefunctions. Akin to topological insulators, this non-trivial wavefunction topology results in various types of protected zero-energy states at the edge or surface of noncentrosymmetric superconductors [1-3].

For instance, a fully gapped noncentrosymmetric superconductor with nontrivial topology supports linearly dispersing helical Majorana modes at its boundary [1]. In three-dimensional systems, the stability of these Majorana surface states is protected by an integer ($\mathbb{Z}$) topological invariant, i.e., the three-dimensional winding number [1], whereas in two-dimensional systems a binary ($\mathbb{Z}_2$) topological number guarantees the robustness of the edge modes. Topologically protected zero-energy boundary modes also occur in noncentrosymmetric superconductors with line nodes. In particular, we have recently shown that dispersionless zero-energy states (i.e., flat bands) of topological origin generically appear at the surface of three-dimensional nodal noncentrosymmetric superconductors [1,2]. These zero-energy flat bands are confined to regions of the two-dimensional surface Brillouin zone that are bounded by the projections of the nodal lines of the bulk gap (see Figs. 1 and 2). Apart from these two-dimensional surface flat bands, certain nodal noncentrosymmetric superconductors also support zero-energy boundary states that form one-dimensional open arcs in the surface Brillouin zone, connecting the projection of two nodal rings [3] [see Figs. 1(a) and 2(a)]. Moreover, we have also shown that Majorana surface states can occur at time-reversal-invariant momenta of the surface Brillouin zone, even if the superconductor is not fully gapped in the bulk [1,3].

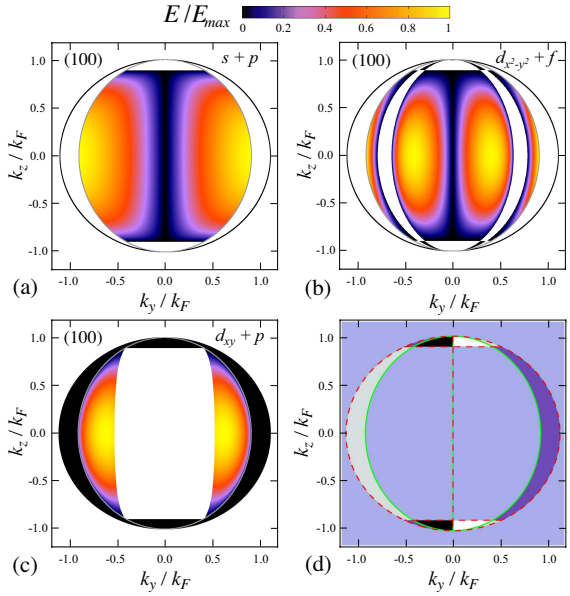

Figure 1: Surface bound-state spectra at the (100) face of a C_{4v} point-group noncentrosymmetric superconductor as a function of surface momentum $\mathbf{k}_{\parallel} = (k_y, k_z)$ with (a) $(s+p)$-wave, (b) $(d_{x^2-y^2}+f)$-wave, and (c) $(d_{xy}+p)$-wave pairing symmetry. The color scale indicates the energy: black represents zero energy while yellow represents the maximum energy $E_{\rm max}$. The black (gray) line shows the extent of the projected negative-helicity (positive-helicity) Fermi surface. (d) Winding number $W_{(100)}$, Eq. (2), at the (100) face corresponding to the same parameters as in panel (c). Black (white) indicates $W_{(100)} = +2$ (-2), dark blue (gray) corresponds to $W_{(100)} = +1$ (-1), while light blue is $W_{(100)} = 0$. The red dashed (green solid) lines represent the nodal lines on the negative-helicity (positive-helicity) Fermi surface.

The topological protection of these zero-energy states that appear at the surface of nodal noncentrosymmetric superconductors is linked to the topological characteristics of the nodal gap structure via a bulk-boundary correspondence. In fact, the stability of both the zero-energy surface states and the line nodes of the bulk gap is ensured by the conservation of the same topological invariants. For example, the stability of the nodal lines is

[1]Technische Universität Dresden, Germany
[2]University of Illinois, USA

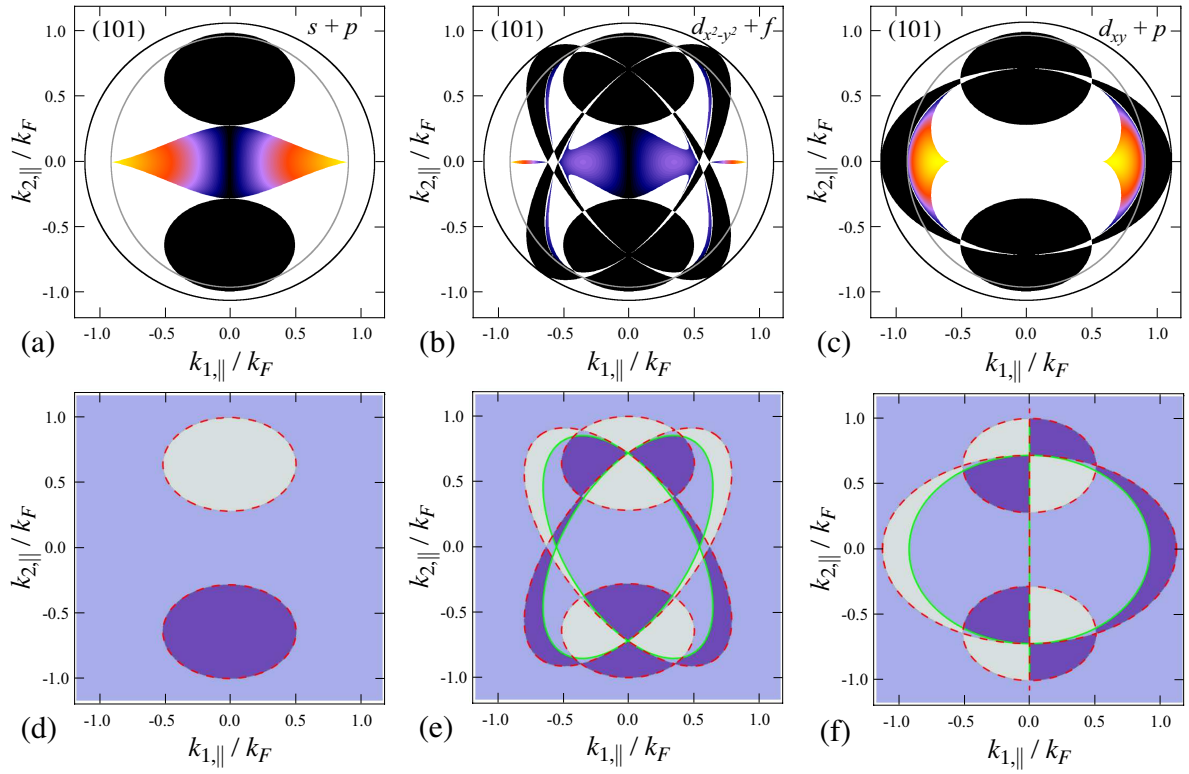

Figure 2: Surface bound-state spectra at the (101) face of a C_{4v} point-group noncentrosymmetric superconductor as a function of surface momentum $\mathbf{k}_\parallel$ with (a) $(s+p)$-wave, (c) $(d_{x^2-y^2}+f)$-wave, and (e) $(d_{xy}+p)$-wave pairing symmetry. The color scale is the same as in Figs. 1(a)–(c). The black (gray) line shows the extent of the projected negative-helicity (positive-helicity) Fermi surface. Panels (b), (d), and (f) show the winding number $W_{(101)}$ at the (101) face corresponding to the same parameters as in panels (a), (c), and (e), respectively. Dark blue (gray) indicates $W_{(101)}=+1\,(-1)$, while light blue is $W_{(101)}=0$. The red dashed (green solid) lines represent the nodal lines on the negative-helicity (positive-helicity) Fermi surface.

protected by the one-dimensional winding number

$$W_{\mathcal{L}} = \frac{1}{2\pi}\oint_{\mathcal{L}} dk_l\,\partial_{k_l}\Big[\arg\left(\xi^+_{\mathbf{k}}+i\Delta^+_{\mathbf{k}}\right) + \arg\left(\xi^-_{\mathbf{k}}+i\Delta^-_{\mathbf{k}}\right)\Big], \tag{1}$$

where the integral is to be evaluated along the path $\mathcal{L}$ parametrized by k_l. Here, $\xi^\pm_{\mathbf{k}}$ is the dispersion of the positive-helicity and negative-helicity bands, respectively, and $\Delta^\pm_{\mathbf{k}}$ denotes the gaps on the two helicity bands. If $\mathcal{L}$ in Eq. (1) encircles a line node, then $W_{\mathcal{L}}$ determines the topological charge and hence the topological stability of the nodal line. The stability of the surface flat band is protected by the very same topological number, namely, by

$$W_{(lmn)}(\mathbf{k}_\parallel) = \frac{1}{2\pi}\int dk_\perp\,\partial_{k_\perp}\Big[\arg\left(\xi^+_{\mathbf{k}}+i\Delta^+_{\mathbf{k}}\right) + \arg\left(\xi^-_{\mathbf{k}}+i\Delta^-_{\mathbf{k}}\right)\Big], \tag{2}$$

where the subscript (lmn) parametrizes the direction perpendicular to the surface plane and $\mathbf{k}_\parallel$ ($\mathbf{k}_\perp$) denotes the momentum parallel (perpendicular) to the surface. At a given surface momentum $\mathbf{k}_\parallel$, there appear zero-energy surface states whenever $W_{(lmn)}(\mathbf{k}_\parallel)\neq 0$. The integral (1) can be related to the integral (2) by considering a suitable deformation of the integration path. By such a construction, one can show that the zero-energy flat bands are confined to regions of the surface Brillouin zone that are bounded by the projections of the nodal lines of the bulk gap.

Beside the integer topological charge (1), nodal lines in noncentrosymmetric superconductors can also carry a binary ($\mathbb{Z}_2$) topological charge determined by the so-called two-dimensional $\mathbb{Z}_2$ topological invariant. We have shown in Ref. [3] that this $\mathbb{Z}_2$ topological charge gives rise to one-dimensional arcs of zero-energy surface states,

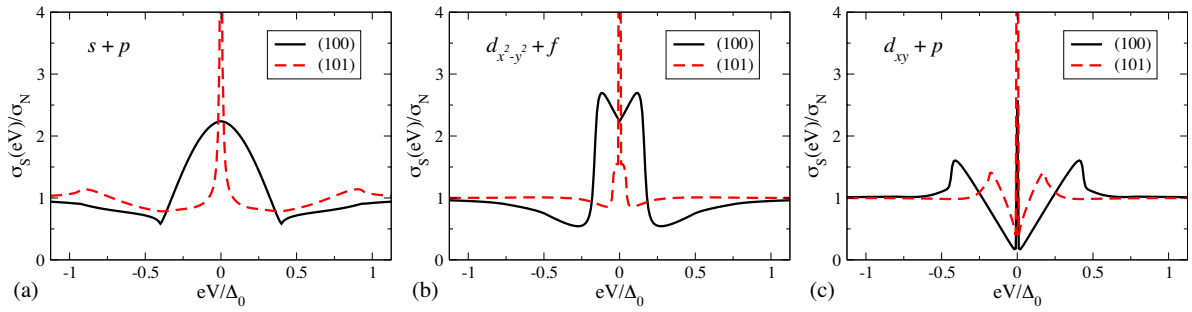

Figure 3: Tunneling conductance spectra for the (100) and (101) interfaces of a C_{4v} noncentrosymmetric superconductor with (a) $(s+p)$-wave gap symmetry, (b) $(d_{x^2-y^2}+f)$-wave gap symmetry, and (c) $(d_{xy}+p)$-wave gap symmetry.

terminating at the projection of the nodal lines onto the surface Brillouin zone. Finally, noncentrosymmetric superconductors can also support Majorana surface states, whose stability is guaranteed by the so-called one-dimensional $\mathbb{Z}_2$ topological number [2,3].

In Fig. 1 we illustrate the topologically protected surface states for the (100) face of a C_{4v} point-group noncentrosymmetric superconductor for several different pairing symmetries. In the case of $(s+p)$-wave pairing and $(d_{x^2-y^2}+f)$-wave pairing we observe zero-energy arc surface states connecting the projections of two nodal rings [see Figs. 1(a) and 1(b)]. In contrast, for $(d_{xy}+p)$-wave pairing we do not find any arc surface states, but instead there are zero-energy flat bands in several regions bounded by the projected line nodes of the positive-helicity and negative-helicity gaps [see Fig. 1(c)]. The zero-energy states lying outside the projected positive-helicity Fermi surface (gray line) are associated with a non-trivial winding number $W_{(100)} = \pm 1$ as shown in Fig. 1(d). The zero-energy surface states lying inside the projected positive-helicity Fermi surface, on the other hand, are doubly degenerate and have winding number $W_{(100)} = \pm 2$. The latter states occur in the region where the gap has predominantly singlet character, and hence are due to the same mechanism as the zero-energy surface states in a pure d_{xy}-wave superconductor.

The bound states at the (101) surface shown in Fig. 2 display a much more interesting topological character. For the $(s+p)$-wave case [Fig. 2(a)] we find that flat zero-energy bands occur within the projected nodes of the negative-helicity Fermi surface. These zero-energy states are associated with a finite winding number $W_{(101)} = \pm 1$ [see Fig. 2(d)]. Besides the surface flat bands there are also arc surface states which connect the projections of the topologically charged nodal rings. The presence of higher angular-momentum harmonics [Figs. 2(b) and 2(c)] results in the appearance of additional regions of zero-energy states due to the nodes of both the positive-helicity and negative-helicity gaps. All of these states correspond to a winding number of $W_{(101)} = \pm 1$, as can be seen by comparing the bound state spectra, Figs. 2(b) and 2(c), with the winding number calculations, Figs. 2(e) and 2(f), respectively.

Let us now examine the signatures of the arc surface states and of the zero-energy surface flat bands in tunneling-conductance spectra. In Fig. 3 we present the conductance spectra for tunneling into a C_{4v} point-group noncentrosymmetric superconductor through (100) and (101) interfaces for $(s+p)$-wave, $(d_{x^2-y^2}+f)$-wave, and $(d_{xy}+p)$-wave pairing symmetry. Several features of these spectra are noteworthy. For the (100) surface we observe a broad hump-like feature in the tunneling conductance for the $(s+p)$-wave and $(d_{x^2-y^2}+f)$-wave pairing states, which is a signature of the arc surface states. In the $(d_{xy}+p)$-wave case, in contrast, we find a zero-bias conductance peak well separated from the bulk density of states. For the (101) surface all pairing symmetries show a zero-bias conductance peak, which is a key experimental signature of the topologically protected surface flat band. For the cases of $(s+p)$-wave and $(d_{x^2-y^2}+f)$-wave pairing, however, we note that the zero-bias conductance peak is superimposed on a hump-like feature. This signals the continued existence of arc surface states in these systems, in agreement with Fig. 2.

To summarize, the topologically protected surface flat bands manifest themselves in scanning tunneling spectroscopy as a zero bias conductance peak, while the arc surface states lead to a broad, hump-like feature centered around zero bias in the conductance spectra. Both features exhibit a pronounced dependence on surface orientation, which not only provides characteristic fingerprints of the orbital and spin pairing symmetries in these materials, but also directly evidences the topological properties of the system. Besides the tunneling conductance, the surface flat bands and arc surface states also profoundly affect other surface and interface properties of NCSs, such as Josephson tunneling, the nonlinear Meissner effect, and surface thermal transport. The investigation of these interesting boundary properties are left for future work.

References:

[1] *Schnyder, A. P. and S. Ryu.* Physical Review B **84**, 060504(R) (2011).

[2] *Brydon, P. M. R., A. P. Schnyder, and C. Timm.* Physical Review B **84**, 020501(R) (2011).

[3] *Schnyder, A. P., P. M. R. Brydon, and C. Timm.* Physical Review B **85**, 024522 (2012).